

Shot Noise Suppression at Non-integer Conductance Plateaus in a Quantum Point Contact

N. Y. Kim,^{*} W. D. Oliver,[†] and Y. Yamamoto[‡]
*Quantum Entanglement Project, ICORP, JST,
E. L. Ginzton Laboratory, Stanford University,
Stanford, California 94305*

Y. Hirayama
*NTT Basic Research laboratories, 3-1 Morinosato-Wakamiya
Atsugi, Kanagawa, 243-01 Japan*
(Dated: November 19, 2003)

We study non-equilibrium differential conductance and current fluctuations in a single quantum point contact. The two-terminal electrical transport properties – differential conductance and shot noise – are measured at 1.5 K as a function of the drain-source voltage and the Schottky split-gate voltage. In differential conductance measurements, conductance plateaus appear at integer multiples of $2e^2/h$ when the drain-source voltage is small, and the plateaus evolve to a fractional of $2e^2/h$ as the drain-source voltage increases. Our shot noise measurements correspondingly show that the shot noise signal is highly suppressed at both the integer and the non-integer conductance plateaus. This main feature can be understood by the induced electrostatic potential model within a single electron picture. In addition, we observe the 0.7 structure in the differential conductance and the suppressed shot noise around 0.7 ($2e^2/h$); however, the previous single-electron model cannot explain the 0.7 structure and the noise suppression, suggesting that this characteristic relates to the electron-electron interactions.

PACS numbers: 73.23.Ad, 73.40.Cg, 73.40.Kp, 73.61.Ey

A quantum point contact (QPC) in a two-dimensional electron gas (2DEG) system has been a prototypical device used to investigate low-dimensional mesoscopic physics. The Landauer-Büttiker formalism^{1,2}, which interprets the electrical transport in such devices, is the most widely used theoretical model. By applying a negative voltage to lithographically patterned Schottky gates on top of 2DEG, additional spatial confinements can be achieved. Combinations of QPCs form zero-dimensional quantum dots³ in which single charge tunnelling occurs, and a single QPC defines one-dimensional conducting channels⁴. In the latter situation, the QPC becomes an electron waveguide that regulates the number of transverse modes between electron reservoirs. As a manifestation, a conductance trace consists of quantized steps in integer multiples of the spin degenerate quantum unit of conductance, $G_Q = 2e^2/h$, where e is an electron charge and h is Planck's constant. Recently, the quantum modes of coherent electrons under QPCs were imaged with atomic force microscopy⁵. An additional remarkable feature has been identified around $0.7 G_Q$, which is called the “0.7 structure” or “0.7 anomaly” in the QPC conductance⁶. Its physical origin is still under investigation in terms of the interaction⁷ and spin properties of electrons⁸ by means of conductance.

The integer-plateau picture is true when a drain-source voltage (V_{ds}) is kept small. As V_{ds} increases, the plateaus evolve from integer units nG_Q to non-integer units $(\beta + n)G_Q$, where β is a fraction between 0 and 1 and n is a non-negative integer⁹. The transition of

conductance plateaus can be understood by a model of an electrostatic potential which is a function of V_{ds} ^{10,11}. Due to the discrepancy between the number of allowed forward and backward transverse modes for a given finite energy window, the location of quantized levels depends on the degree (β) of the voltage drop across drain and source sides.

Along with experimental and theoretical work on the conductance, the current fluctuations have been studied as well with QPCs since these fluctuations provides information that is not contained, even in principle, in the conductance. Shot noise is the non-equilibrium current fluctuation resulting from the stochastic transport of quantized charge carriers. In mesoscopic conductors, shot noise occurs due to the random partition of electrons by a scatterer. Previous shot noise experiments with a QPC^{12,13} clearly showed that shot noise signals agree well with a non-interacting theory, meaning that shot noise is nearly zero at the integer conductance plateaus where electrons are fully transmitted. We, however, have not yet found any thorough noise studies on the characteristic around the 0.7 structure clearly seen in early noise data^{14,15} except as reported in the Ph.D. thesis¹⁶ regarding to such structure.

In this Letter, we reexamine a single QPC and report our experimental results on low frequency shot noise as well as differential conductance at 1.5 K by sweeping both V_{ds} and a split-gate voltage V_g . We find a close connection between noise and conductance data. Shot noise is suppressed when conductance approaches quantized val-

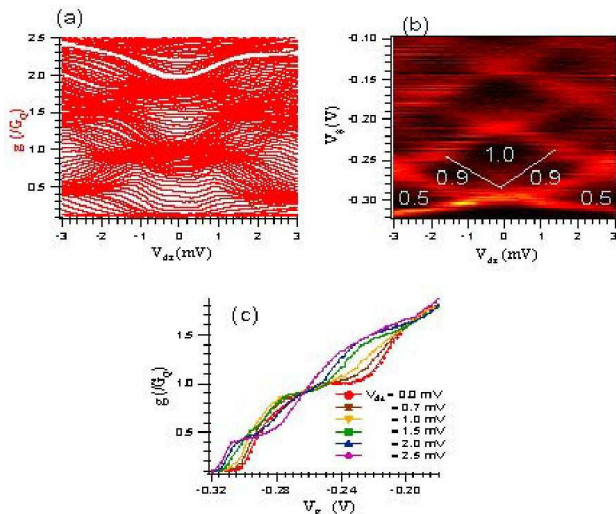


FIG. 1: (Color online) (a) Differential conductance $g = dI/dV_{ds}$ as a function of V_{ds} normalized by $G_Q = 2e^2/h$ at 1.5 K. (b) Transconductance dg/dV_g obtained by mathematical analysis. Black color indicates plateaus in (a) and red represents transitions between plateaus. The first big black diamond region can be divided into three sections; the top is from G_Q plateau and the bottom two are related to the $0.9 G_Q$ plateaus. (c) The traces of g for various V_{ds} versus V_g .

ues of G_Q . Furthermore, the highly reduced shot noise signals are resolved near other fractional G_Q regions and around $0.7 G_Q$ for non-zero V_{ds} .

Our QPC devices were fabricated on a high mobility 2DEG formed in an undoped GaAs/AlGaAs heterostructure. A back-gate field-effect configuration allows us to tune the electron density in 2DEG¹⁸. The average electron density is $2 \times 10^{11} \text{ cm}^{-2}$. From the Hall bar pattern, the voltage drop across the QPC can be probed so that QPC conductance was experimentally extracted. Two external parameters — V_{ds} and V_g — were varied in both the differential conductance, $g = dI/dV_{ds}$, and the low frequency two-terminal shot noise measurements. A standard lock-in technique was used on the differential conductance g measurement. In order to improve the signal-to-noise-ratio in the shot noise experiment, an ac modulation lock-in technique and a resonant circuit were used together with a home-built cryogenic low-noise preamplifier^{12,14,17}. All measurements were performed in a He³ cryostat, whose base temperature was kept at 1.5 K.

The measured differential conductance g with an ac bias voltage $V_{ac} \sim 100 \mu\text{V}$ is plotted as a function of V_{ds} and V_g in Fig. 1(a). All data on each line are taken at a different V_g , and all measured values are normalized by G_Q . Dark regions are formed around the regions of plateaus. Conductance flattens around G_Q and $2 G_Q$ along $V_{ds} \sim 0$, but away from $V_{ds} \sim 0$, g approaches plateaus at different locations. Alternatively, Fig. 1(c) clearly illustrates that the first step appears below $0.5 G_Q$ when $V_{ds} = -2.5 \text{ mV}$. We compute transconductance

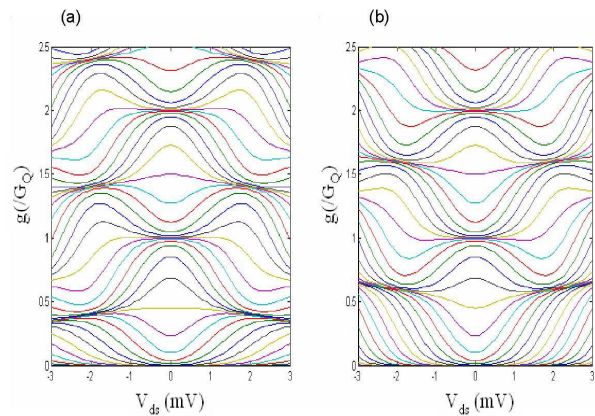


FIG. 2: The calculated differential conductance g based on the saddle-point potential model which has both a linear and a quadratic term of V_{ds} . The sign of γ determines the manner of the plateau evolution for a finite V_{ds} : (a) a negative quadratic term (decreasing plateaus)(b) a positive quadratic term (increasing plateaus). Assuming a symmetric barrier, β is chosen as $1/2$ and U_y/U_x is set to 2. Given a fixed value of γ , the same plot as the measurement data cannot be generated.

dg/dV_g by differentiating g in terms of V_g , and plot it in a two-dimensional image graph (Fig. 1(b)). Here, black areas correspond the plateaus due to the small difference between traces along V_g axis. In the first big diamond black area, there is a V-shape red structure, which separates the $0.9 G_Q$ structures from the G_Q plateau.

Furthermore, we notice that the transition behavior is not identical over the whole conductance values for finite V_{ds} . Below G_Q , an additional shoulder structure around $0.7 G_Q$ is manifest and it moves to $0.9 G_Q$, and then the plateau clearly forms below $0.5 G_Q$ at a large V_{ds} . In contrast, above G_Q , as V_{ds} increases, no structure similar to the 0.7 anomaly is apparent and the plateau shows an increasing manner. The appearance of the non-integer conductance plateaus in terms of V_{ds} is understood quantitatively by a V_{ds} -dependent saddle-point potential where the potential in a two-dimensional x and y plane is given by¹⁰

$$U(x, y) = U_0(V_{ds}) + U_y y^2 - U_x x^2.$$

The first term in the right hand side contains the effect of a non-zero V_{ds} and it is written as:

$$U_0(V_{ds}) = U_0 - \beta e V_{ds} + \gamma e V_{ds}^2/2,$$

where the coefficient β is determined by the actual voltage drop between the drain and source side, and γ is related to the trend of plateau movements as V_{ds} gets bigger¹⁰.

Although the simulation result (Fig. 2) show the qualitative picture of plateau evolution in V_{ds} , it fails to replicate the $0.7 G_Q$ and $0.9 G_Q$ structures, suggesting that more complicated physical mechanism is involved under G_Q and especially around $0.7 G_Q$ and $0.9 G_Q$.

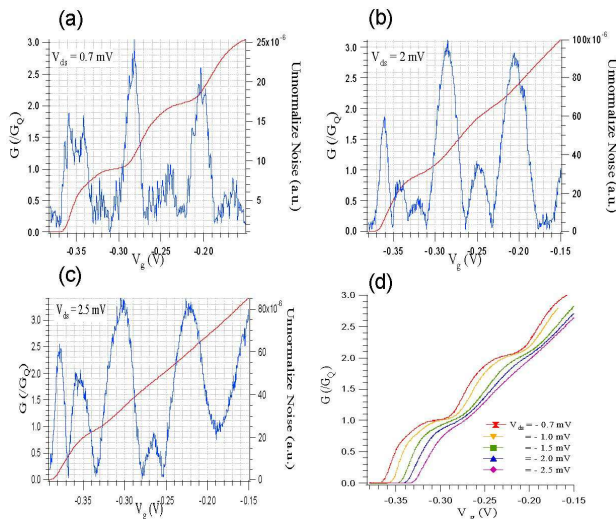


FIG. 3: (Color online) Shot noise (blue: the right vertical axis scale) and conductance $G = I/V_{ds}$ (Red: the left vertical axis scale) for various V_{ds} (a) 0.7 mV (b) 2 mV and (c) 2.5 mV. (d) V_g dependence of conductance G . For clarity, the traces are shifted along V_g axis.

Following the differential conductance experiments, the low frequency two-terminal shot noise measurements performed. In order to extract the distinguishable shot noise signal from background noise, V_{ds} cannot be smaller than $500 \mu V$. Three representative graphs are drawn as a function of V_g in Fig. 3. Similar behaviors were observed in other devices as well. No matter what value of V_{ds} was applied, the shot noise level was clearly minimal when conductance $G = I/V_{ds}$ reached about G_Q and $2 G_Q$. The degree of the suppression at $3 G_Q$ became less smaller for a large V_{ds} . In the transient zones between the multiples of G_Q , the noise characteristic was rather complex. Below the first plateau, the noise suppression appeared around $0.6 G_Q$ and $0.9 G_Q$ until $V_{ds} \sim 1.5$ mV (Fig. 3(a)). As V_{ds} further increased, these locations moved down to $0.5 G_Q$ and $0.8 G_Q$ (Fig. 3(b)), and eventually the suppressed noise was found only at $0.4 G_Q$ for $V_{ds} > 2.5$ mV (Fig. 3(c)). Unlikely, when G is higher than G_Q , only one additional noise reduction was found about $1.6 G_Q$ or $1.7 G_Q$ regardless of the magnitude of V_{ds} . Meanwhile, the plateau structures in G gradually washed out as V_{ds} increased as shown in Fig. 3(d).

Figure 4 (a) exhibits the above observation of the shot noise response as a function of V_{ds} and V_g in a continuous manner. The black color depicts the base shot noise level. Even though the occurrence of the suppressed shot noise can be easily seen in units of G_Q , the actual plot contains other noticeable features. The colored contour plot of conductance $G = I/V_{ds}$ (Fig. 4(b)) helps us to see the relation of G and the shot noise. Again under G_Q , several black strips are visible: The upper strip relates to the shot noise suppression around G_Q , and the lower two ones start at the conductance values $0.7 G_Q$ and $0.9 G_Q$. For a high V_{ds} , the shot noise suppression occurs at less

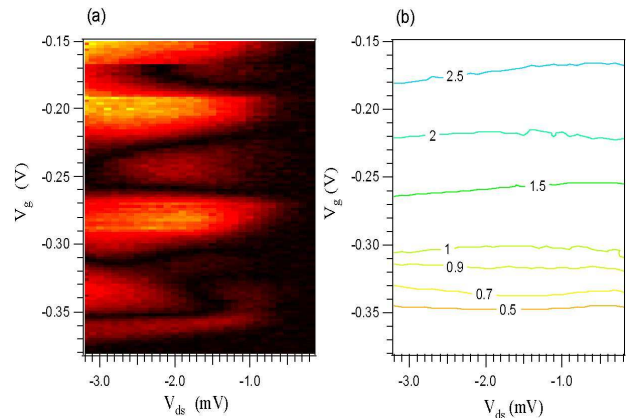


FIG. 4: (Color online) (a) Shot noise is plotted as a function of both V_{ds} and V_g . Dark region represents suppressed noise level. (b) The contour map of corresponding conductance G . The numbers represent normalized conductance values by G_Q .

than $0.5 G_Q$. The shot noise signal in higher G has a rather simple pattern: The reduced noises are observed around 1.6 or $1.7 G_Q$ and $2 G_Q$ as previously stated.

We notice that the shot noise behavior in the transient zone between the integer multiples of G_Q shares some features with the transconductance two-dimensional image plot (Fig. 1(b)). The peaks in the transconductance correspond to the larger shot noise signals and the dark areas in the transconductance match to the black strips in the shot noise image. Moreover, both the transconductance and the shot noise share common features for $G < G_Q$; 0.7 structure can be distinctive and the location of the noise suppression and the new plateaus in dg/dV_g occur around $0.4 G_Q$ as $V_{ds} > 2$ mV. Within the saddle-point potential model, dg/dV_g is expressed in terms of $T_i(1 - T_i)$ where T_i is the i -th one-dimensional (1D) channel transmission probability. Since the shot noise has a term of $T_i(1 - T_i)$ for a small energy window, two quantities are closely related. It is not, however, obvious to predict the response of the shot noise for a large V_{ds} because the shot noise is obtained from the integral of the energy dependent transmission probability. Qualitatively, the noise suppression around the plateaus can be expected based on the fact that the current fluctuations can be zero or low when the current remains constant.

The different characteristics in both the transconductance and the shot noise are observed in the region of $G < G_Q$ and $G > G_Q$. This observation is certainly beyond the simple saddle-point potential model in a single-particle approximation. In particular, it is surprising to have the strongly suppressed shot noise at $0.7 G_Q$, meaning that electrons are regulated by a certain governing physical mechanism. The possible factor relating to the mechanism of the 0.7 anomaly would be the density of electrons. The shot noise study in terms of the electron density would provide more information to explore this question in the future.

In conclusion, we have experimentally studied the low frequency shot noise and the differential conductance with finite values of V_{ds} . We showed that the main feature of shot noise suppression in terms of V_{ds} can be understood by the differential conductance. However, the further investigation of the properties of both the dif-

ferential conductance and the shot noise around the 0.7 structure should be needed in order to establish better understandings.

We acknowledge the ARO-MURI grant DAAD19-99-1-0215 for supporting this research.

* Corresponding author.; Email: nayoung@stanford.edu

† Present address: MIT Lincoln Laboratory, Lexington, Massachusetts, 02420

‡ also at NTT Basic Research Laboratories, 3-1 Morinosato-Wakamiya Atsugi, Kanagawa, 243-01 Japan

¹ M. Büttiker, Phys. Rev. B **46**, 12485 (1992).

² Th. Martin and R. Landauer, Phys. Rev. B **45** 1742 (1992).

³ M. A. Kastner, Physics Today **46**(1), 24 (1993).

⁴ H. van Houten and C. Beenakker, Physics Today **49**(7), 22 (1996).

⁵ M. A. Topinka, B. J. LeRoy, R. M. Westervelt, S. E. J. Shaw, R. Fleischmann, E. J. Heller, K. D. Maranowski, and A. C. Gossard, Nature **410**, 183 (2001).

⁶ *Recent review* R. Fitzgerald, Physics Today **55**(5), 21 (2002).

⁷ K. J. Thomas, J. T. Nicholls, M. Y. Simmons, M. Pepper, D. R. Mace, and D. A. Ritchie, Phys. Rev. Lett. **77**, 135 (1996).

⁸ S. M. Cronenwett, H. J. Lynch, D. Goldhaber-Gordon, L. P. Kouwenhoven, C. M. Marcus, K. Hirose, N. S. Wingreen, and V. Umansky, Phys. Rev. Lett. **88**, 226805

(2002).

⁹ N. K. Patel, J. T. Nicholls, L. Martin-Moreno, M. Pepper, J. E. F. Frost, D. A. Ritchie, and G. A. C. Jones, Phys. Rev. B **44**, 13549 (1991).

¹⁰ L. Martin-Moreno, J. T. Nicholls, N. K. Patel, and M. Pepper, J. Phys.:Condens. Matter **4**, 1323 (1992).

¹¹ L. P. Kouwenhoven, B. J. van Wees, C. J. P. M. Harmans, J. G. Williamson, H. van Houten, C. W. J. Beenakker, C. T. Foxon, and J. J. Harris, Phys. Rev. B **39**, 8040 (1989).

¹² M. Reznikov, M. Heiblum, H. Shtrikman, and D. Mahalu, Phys. Rev. Lett. **75**, 3340 (1995).

¹³ A. Kumar, L. Saminadayar, D. C. Glatli, Y. Jin, and B. Etienne, Phys. Rev. Lett. **76**, 2778 (1996).

¹⁴ R. C. Liu, B. Odom, Y. Yamamoto, and S. Tarucha, Nature **391**, 263 (1998).

¹⁵ M. Heiblum (Private communication)

¹⁶ W. D. Oliver, Ph.D. Dissertation (2002).

¹⁷ W. D. Oliver, J. Kim, R. C. Liu, and Y. Yamamoto, Science **284**, 299 (1999).

¹⁸ Y. Hirayama and Y. Tokura (Private communication)